DEPARTMENT OF ELECTRONICS AND COMMUNICATION ENGINEERING

ANIL NEERUKONDA INSTITUTE OF TECHNOLOGY AND SCIENCES

(*Permanently Affiliated to AU, Approved by AICTE and Accredited by NBA & NAAC with 'A' Grade*)

Sangivalasa, bheemilimandal, visakhapatnamdist.(A.P)

PRAGNANAM BRAHMA

ANITS

CERTIFICATE

This is to certify that the project report entitled "**X-RAY BIO-IMAGE DENOISING USING DIRECTIONAL-WEIGHTED-MEAN FILTERING AND BLOCK MATCHING APPROACH**" submitted by **M. Sai krishna (318126512030), A. Sri Ragamayi (318126512004), M. Gowtham (318126512029), V. Roop Sai Sakthi Kumar (318126512045)** in partial fulfillment of the requirements for the award of the degree of **Bachelor of Engineering in Electronics & Communication Engineering** of Andhra University, Visakhapatnam is a record of bonafide work carried out under my guidance and supervision.

Project Guide

Mr. Bibekananda Jena
M. Tech (Ph.D.)
Asst. Professor
Department of E.C.E
ANITS

Assistant Professor
Department of E.C.E.
Anil Neerukonda
Institute of Technology & Sciences
Sangivalasa, Visakhapatnam-531 162

Head of the Department

Dr. V. Rajyalakshmi
M.E,Ph.D.,MIEEE,MIETE,MIE
Professor
Department of E.C.E
ANITS

Head of the Department
Department of E C E
Anil Neerukonda Institute of Technology & Sciences
Sangivalasa-531 162

ACKNOWLEDGEMENT

We would like to express our deep gratitude to our project guides **Mr. Bibekananda Jena,** Asst. professor, Department of Electronics and Communication Engineering, ANITS, for his/her guidance with unsurpassed knowledge and immense encouragement. We are grateful to **Dr. V. Rajyalakshmi**, Head of the Department, Electronics and Communication Engineering, for providing us with the required facilities for the completion of the project work.

We are very much thankful to the **Principal and Management, ANITS, Sangivalasa,** for their encouragement and cooperation to carry out this work.

We express our thanks to all **teaching faculty** of Department of ECE, whose suggestions during reviews helped us in accomplishment of our project. We would like to thank **all non-teaching staff** of the Department of ECE, ANITS for providing great assistance in accomplishment of our project.

We would like to thank our parents, friends, and classmates for their encouragement throughout our project period. And last but not the least, we thank everyone for supporting us directly or indirectly in completing this project successfully.

PROJECT STUDENTS

M. Sai Krishna(318126512030)

A. Sri Ragamayi(318126512004)

M. Gowtham (318126512029)

V. Roop Sai Sakthi Kumar (318126512045)

CONTENTS

CHAPTER -7: EXPERIMENTAL RESULTS AND ANALYSIS

7.1 Experimental Structure

7.2 Experimental Analysis on Standard Images

7.3 Experimental Analysis on Medical Images

7.4 Result Analysis

CHAPTER -8: DISCUSSIONS AND REFERENCES

CHAPTER- 9: CONCLUSION

Abstract

An X-ray bio-image might suffer interference from salt-and-pepper (SAP) noise during transmission or capture, thus reducing image quality. This project includes a three-stage method to cope with this problem. A directional-weighted-mean (DWM) filter is used to take out the corruption noise in the first stage. In the second stage, confirmation of extreme pixels (255 or 0 for an 8-bit grey level bio-image) is performed to restore the X-ray bio-images. In the final stage, block matching identifies blocks with similar textures in a local region. The centre pixels of these similar blocks are then averaged to refine the grey value of the restored pixel, thus allowing improvement to the quality of the restored X-ray image through consideration of the texture properties in neighbor pixels over a large size window. In this project we will efficiently take out background noise from an SAP noise corrupted bio-image for various noise densities. The reconstructed bio-image does not incur blurring even under heavy noise corruption.

OVERVIEW

I. INTRODUCTION

A bio-image might be corrupted by salt-and-pepper (SAP) noise potentially caused by transmission error or sensor malfunction. SAP noise seriously impacts X-ray images[1]. The grey values of noisy pixels are either the maximum value 255 or minimum value 0 for an 8-bit grey level image. Lowquality bio-images increase the difficulty of diagnosis determination. Accordingly, developing an effective approach to restore the SAP noise is important for X-ray image processing They used an adaptive window to detect candidate

noise pixels for modification using they classified pixels into three classes, including noise-free pixels, along with lightly and heavily corrupted pixels. The classification rule rests on the maximum luminance difference of pixels. The grey value of the noisy pixel is modified by the weighted mean value, which is computed separately for light and heavy noise corruption

If the values of all pixels are extreme, the grey value of the centre pixel is modified by the mean value of all pixels in the local window

The size of the masking window is not limited, and proper median values can be found to restore noisy pixels This filter take outs the interference noise by using the median of the significant neighbour pixels, and uses the lifting method in the wavelet domain Noise-corrupted pixels are detected by an adaptive fuzzy method, and the grey levels of noisy pixels are modified by the weighted mean on the noise-free neighbouring pixels. Experiments show that this approach works well against heavy noise corruption This algorithm assigns a membership value to the noise-corrupted neighbour pixels and a grey value for the restoration

. The grey value of a noisy pixel is modified by the weighted median of the pixels on a selected direction with minimum variation. This method only uses four directions. The number of directions is small

The method significantly improved DWM filter, using additional eight directions to determine the direction of pixel variation for denoising.The method significantly improved DWM filter, using additional eight directions to determine the direction of pixel variationfor denoising If the centre pixel of the analysis window is noisy, its grey level is replaced by a weighted value obtained by multiplying the distribution ratio with the mean value of the grey level for each classified group, thus restoring noisy pixels. This method can efficiently take out interference noise in medical images produced by real brain computed tomography and magnetic resonance imaging.

Their study selects non-extreme pixels based on minimum Euclidean distance to the centre pixel of an analysis window. The mean value of these selected pixels is computed to replace the grey

level of the noisy centre pixel, allowing for the noisy pixels to be reconstructed.These studies indicate the importance of efficiently removing SAP noise in images. This paper proposes using a novel three-stage scheme to take out SAP noise from X-ray bio-images. The first stage uses a DWM filter to take out the corruption noise efficiently in a 3 ×3 analysis window. A local window may contain non-extreme and clean pixels which can be used to reconstruct the grey level of noise-corrupted pixels. If the grey values of all pixels are extreme, there are no non-extreme pixels for pixel restoration. Thus, pixel restorationcannot be achieved in this window. [2] The grey value of the centre pixel is determined according to the majority incorporated with bias correction for the black and white pixels in the second stage. To reduce the greyed effect of the original black and white pixels, and thus further improve the quality of the restored X-ray image, the noisy X-ray image is restored in inverse, i.e., the analysiswindow slides from right to left and from top to bottom. An improved version of the restored pixel can be achieved by selecting the smaller grey value of the forward and backward DWM filtered values. The third stage performs block matching to search for blocks withstructures similar to that in the analysis window. The centre pixels of these similar blocks are averaged to replace the restored pixel, thus improving the quality of the restored X-ray image. This improvement is attributed to the consideration of the texture

properties of neighbour pixels inside a large window, thus reducing the grey level variation of similar textures. Finally, the proposed approach could efficiently filter SAP noise from a noisecorrupted bio-image for various levels of noise density. In addition, the denoised bio-image is free from blurring. The major contribution of this study is a block matching method for post processing to improve denoised bio-image quality. Because similar blocks have similar structures in a local region, using the average value of these similar blocks to replace the restored pixels can reduce fluctuation among the post-processed pixels, such as in the areas with smooth variation and on the object edges, thus further improving the visual quality of the restored image

What is an image ?

Is it someone's face, a building, an animal, or anything else?

No, An Image is a multidimensional array of numbers ranging from 0 to 255. Each number can be seen as a combination of x(horizontal) and y(vertical) coordinates, called as pixelAn Image is a spatial representation of a two dimensional or three-dimensional scene.It is an array or a matrix pixel (picture elements) arranged in columns and rows.

An image is also a two-dimensional array specifically arranged in rows and columns. Digital Image is composed of picture elements, image elements, and pixels. A Pixel is most widely used to denote the elements of a Digital Image.

What is a noise?

Noise in an image is the presence of artefacts that do not originate from the original scene content. Generally speaking, noise is a statistical variation of a measurement created by a random process. In imaging, noise emerges as an artefact in the image that appears as a grainy structure covering the image.

Noise can have different forms and appearances within an image and is, in most cases, an unwanted or disturbing artefact that reduces the subjective image quality.

Problem with noise:

Noise is a by product of uneven signal fluctuations that accompany a transmitted signal. What’s important to understand here is that these fluctuations are not a part of the signal and instead obscure the intended target.

Thus, one of the most crucial tasks in imaging is finding a solution to create a strong signal with a minimum amount of noise beside it. Unfortunately, finding a solution often proves to be a significant challenge in imaging, particularly in a low-light situation where the signal is already low. When dealing with image noise, the first step is to identify the type of noise you’re encountering**.**

What is image denoising ?

Image denoising is the technique of removing noise or distortions from an image. There are a vast range of application such as blurred images can be made clear

One of the fundamental challenges in the field of image processing and computer vision is image denoising, where the underlying goal is to estimate the original image by suppressing noise from a noise-contaminated version of the image. Image noise may be caused by different intrinsic (i.e., sensor) and extrinsic (i.e., environment) conditions which are often not possible to avoid in practical situations. Therefore, image denoising plays an important role in a wide range of applications such as image restoration, visual tracking, image registration, image segmentation, and image classification, where obtaining the original image content is crucial for strong performance. While many algorithms have been proposed for the purpose of image denoising, the problem of image noise suppression remains an open challenge, especially in situations where the images are acquired under poor conditions where the noise level is very high.

Types of noises:

- Gaussian noise
- Impulse noise
- Poisson noise
- Speckle noise

- **Gaussian noise:**

Gaussian Noise is a statistical noise having a probability density function equal to normal distribution, also known as Gaussian distribution. Random Gaussian function is added to Image function to generate this noise. It is also called as electronic noise because it arises in amplifiers or detectors.


- **Impulse noise:**

Salt-and-pepper noise, also known as impulse noise, is a form of noise sometimes seen on digital images. This noise can be caused by sharp and sudden disturbances in the image signal. It presents itself as sparsely occurring white and black pixels.

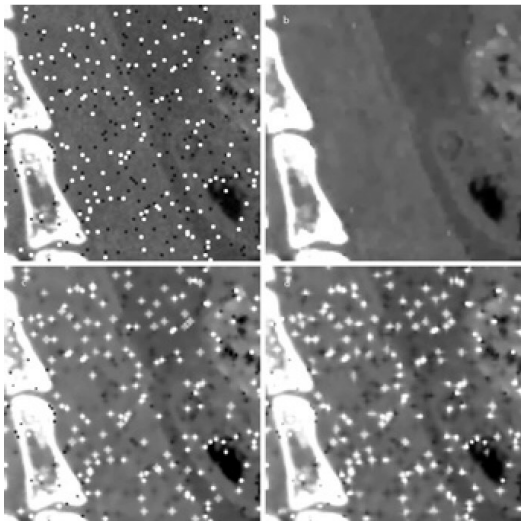

- **Poisson noise:**

These rays are injected in patient's body from its source, in medical x rays and gamma rays imaging systems. These sources are having random fluctuation of photons. Result gathered image has spatial and temporal randomness. This noise is also called as quantum (photon) noise or shot noise.

- **Speckle noise:**

Speckle noise is a multiplicative noise that affects pixels in a grey-scale image, and mainly occurs in low level luminance images such as Synthetic Aperture Radar (SAR) images and Magnetic Resonance Image (MRI) images.

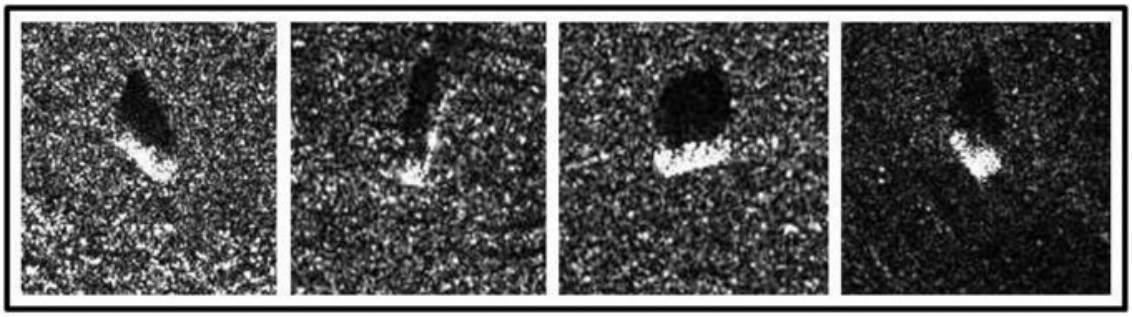

As of our project that we are going to discuss mainly involves "**Impulse noise**" which is of three types namely

- ***Salt noise :***

Salt noise is added to an image by addition of random bright (with 255 pixel value) all over the image

- ***Pepper Noise:***

Pepper noise is added to an image by addition of random dark (with 0 pixel value) all over the image.

- ***Salt and Pepper Noise:***

Salt and Peppernoise is added to an image by addition of both random bright (with 255 pixel value) and random dark (with 0 pixel value) all over the image. This model is also known as data drop noise because statistically it drop the original data values [5]. Source: Malfunctioning of camera's sensor cell.

IMAGE PROCESSING

2.1 INTRODUCTION:

Image processing is a method to perform some operations on an image, in order to get an enhanced image or to extract some useful information from it. It is a type of signal processing in which input is an image and output may be image or characteristics/features associated

with that image. Nowadays, image processing is among rapidly growing technologies. It forms core research area within engineering and computer science disciplines too.

Image processing basically includes the following three steps:

1. Importing the image via image acquisition tools;

2. Analysing and manipulating the image;

3. Output in which result can be altered image or report that is based on image analysis.

Fig 2.1 Example of image processing

TYPES OF IMAGE PROCESSING:

There are two types of methods used for image processing namely:

- **Analogue image processing**:

It can be used for the hard copies like printouts and photographs. Image analysts use various fundamentals of interpretation while using these visual techniques.

- **Digital image processing**:

This technique helps in manipulation of the digital images by using computers. The three general phases that all types of data have to undergo while using digital technique are pre-processing, enhancement, and display, information extraction.

2.2 DIGITAL IMAGE PROCESSING TASKS:

Image Reconstruction

• Removal of system or imaging aberrations.

• Aims to reconstruct the best image from collected data.

• Typically output images for visual inspection.

Image Analysis

• Computer analysis of images.

• Extract features or regions

• Recognition of objects.

• High level pattern recognition.

Image Formation

Image formed by computer

Image Compression and Encoding

• Document and image storage.

Image Representation:

An image defined in the "real world" is considered to be a function of two real variables, for example, f(x,y) with f as the amplitude (e.g. brightness) of the image at the real coordinate position (x,y).

The effect of digitization is shown.

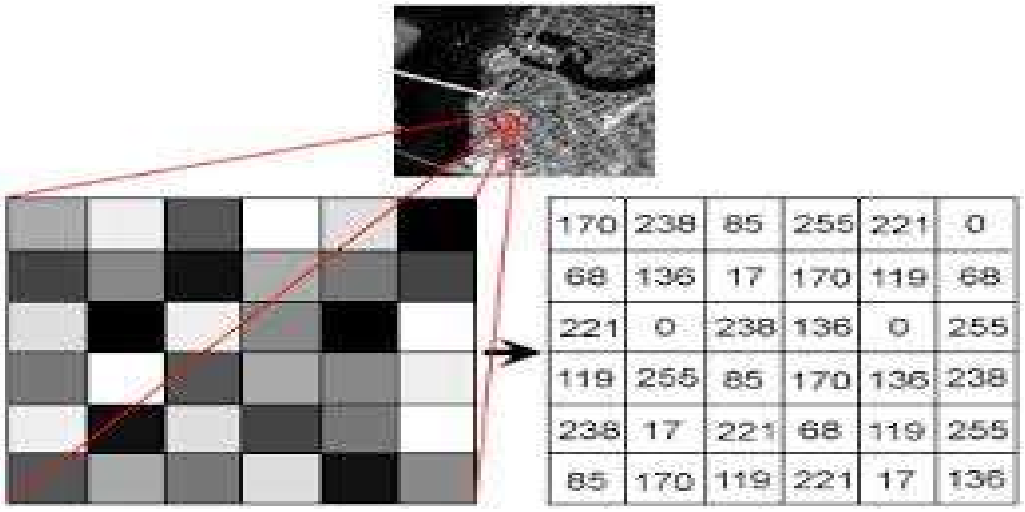

Fig 2.2Effect of digitization

The 2D continuous image f(x,y) is divided into N rows and M columns. The intersection of a row and a column is called as pixel. The value is assigned to the integer coordinates m,n with { m=0,1,2, ….., M-1}and { n=0,1,2,…..,N-1} is f[m,n]. In fact, in most cases f(x,y) which we might consider to be the physical signal that impinges on the face of a sensor. Typically an image file such as BMP, JPEG, TIFF etc., has some header and picture information. A header usually includes details like format identifier (typically first information), resolution, number of bits/pixels, compression type, etc.

IMAGE PROCESSING:

1. Scaling:

The theme of the technique of magnification is to have a closer view by magnifying or zooming the interested part in the imagery. By reduction, we can bring the unmanageable size of data to a manageable limit. For resampling an image Nearest Neighbourhood, Linear, or cubic convolution techniques are used.

2. Magnification:

This is usually done to improve the scale of display for visual interpretation or sometimes to match the scale of one image to another. To magnify an image by a factor of 2, each pixel of the original image is replaced by a block of 2x2 pixels, all with the same brightness value as the original pixel**.**

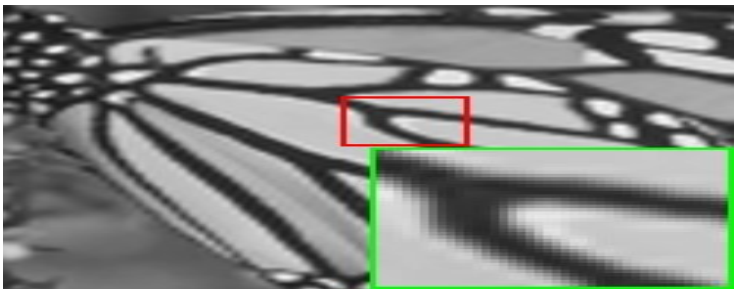

Fig 2.3 Magnification

3. Reduction:

To reduce a digital image to the original data, every mth and nth column of the original imagery is selected and displayed. Another way of accomplishing the same is by taking the average in 'm x m' block and displaying this average after proper rounding of the resultant value.

4. Rotation:

Rotation is used in image mosaic, image registration etc. One of the techniques of rotation in 3-pass shear rotation, where rotation matrix can be decomposed into three separable matrices.

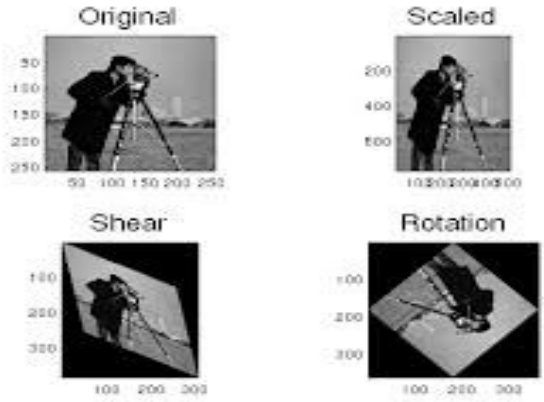

Fig 2.4 Scaling, Rotation

5. Mosaic:

Mosaic is a process of combining two or more images to form a single large image without radiometric imbalance. Mosaic is required to get the synoptic view of the entire area, otherwise capture as small images**.**

6. Contrast stretching:

Some Images dense forests, snow, clouds and under lazy conditions over heterogeneous regions) are homogeneous i.e., they do not have much change in their levels. In terms of histogram representation, they are characterized as the occurrence of very narrow peaks. The homogeneity can also be due to the incorrect illumination of the scene.

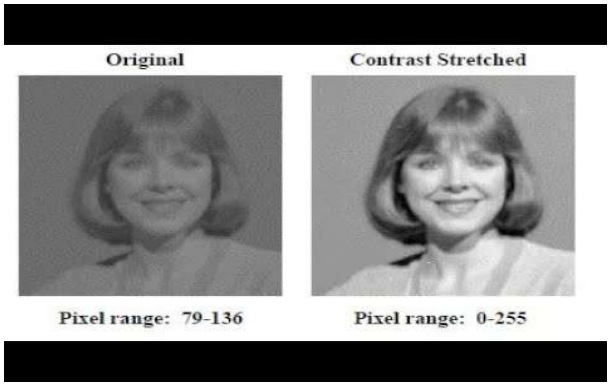

Fig 2.5Contrast stretching

7. Noise Filtering:

Noise filtering is used to filter the unnecessary information from an image. It is also used to take out various types of noises from the images. Mostly this feature is interactive. Various filters like low pass, high pass, mean, median etc., are available.

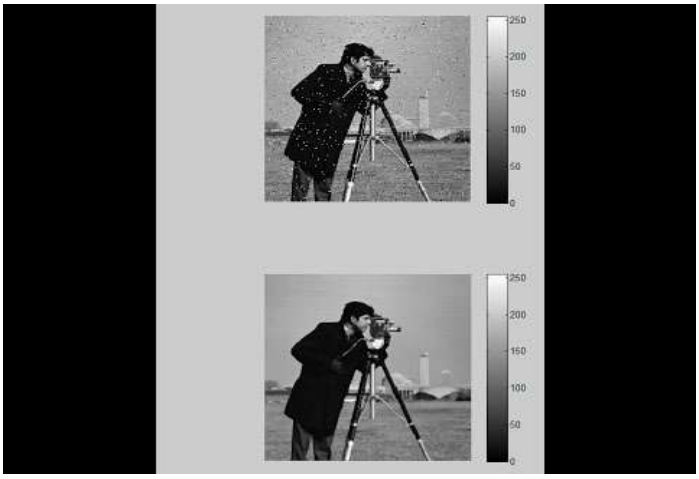

Fig 2.6 Noise Filtering

2.3 ADVANTAGES:

Digital image processing in the most layman terms is image editing to improve it's visual appearance but not limited to it. The main advantages of digital image processing are

1. Digital images can be processed by digital computers.
2. Important features such as edges can be extracted from images which can be
   In industry
3. Images can be given more sharpness and better visual appearance.
4. Minor errors can be rectified.
5. Image sizes can be increased or decreased.
6. Images can be compressed and decompressed for faster image transfer over the network
7. Images can be automatically sorted depending on the contents they have.
8. Unrecognisable features can be made prominent.
9. Images can be smoothened.
10. It allows robots to have vision.
11. It allows industries to take out defective products from the production line.
12. It allows weather forecasting.
13. It is used to analyse cells and their composition.
14. It is used to analyse medical images

2.4 APPLICATIONS:

- Computerized photography (e.g., Photoshop)
- Space image processing (e.g., Hubble space telescope images, interplanetary probe images)
- Medical/Biological image processing (e.g., interpretation of X-ray images, blood/cellular microscope images)
- Automatic character recognition (zip code, license plate recognition)
- Finger print/face/iris recognition
- Remote sensing: aerial and satellite image interpretations
- Reconnaissance

3.1 Flow chart:

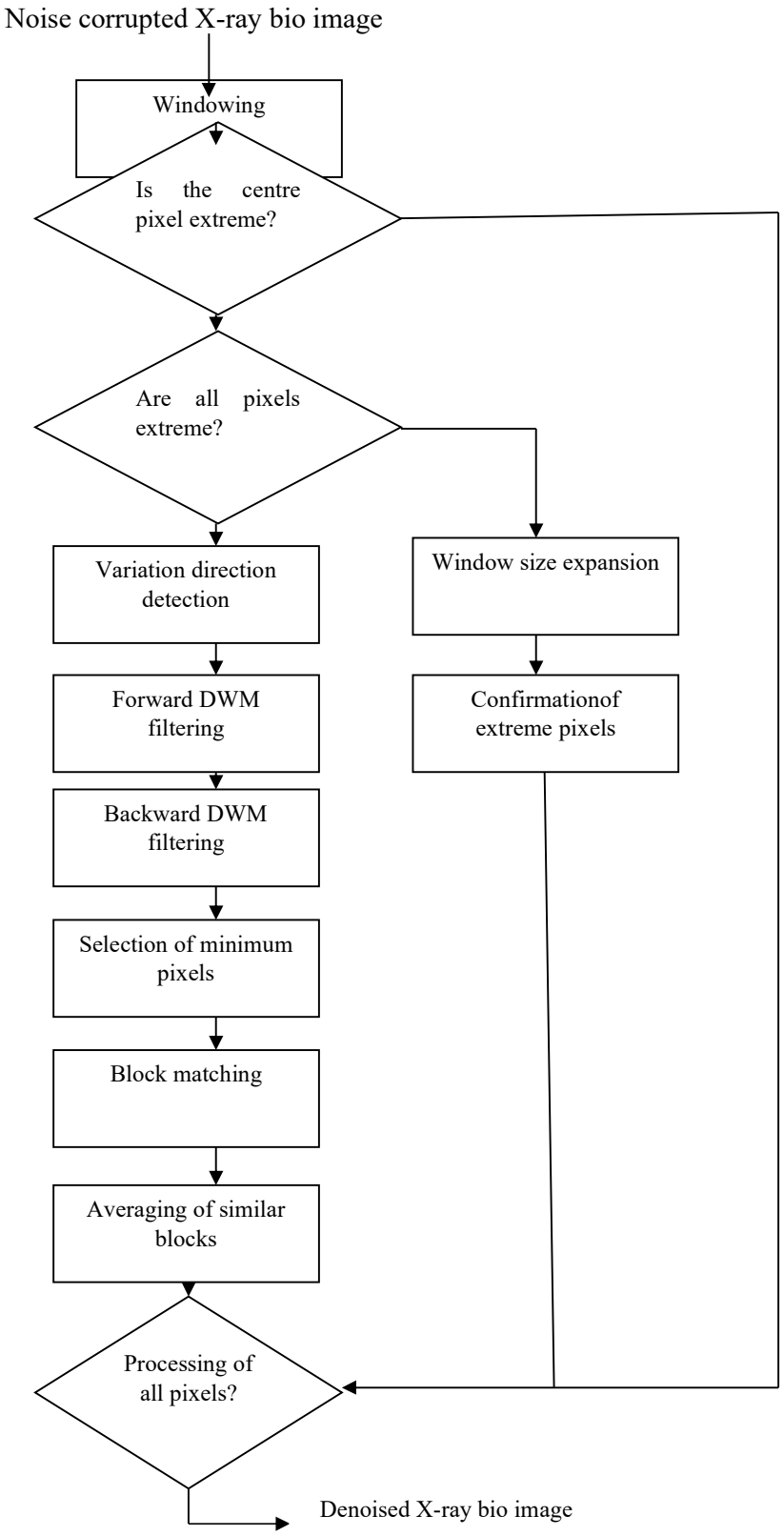

3.2 Windowing:

Image filtering involves the application of window operations that perform useful functions, such as noise removal and image enhancement. This chapter is concerned particularly with what can be achieved with quite basic filters, such as mean, median, and mode filters. Interestingly, these filters have significant effects on the shapes of objects; in fact, the study of shape took place over a long period of time and resulted in a highly variegated set of algorithms and methods, during which the overarching formalism of mathematical morphology was set up.This steers up an intuitive path between the many mathematical theorems, showing how they lead to practically useful techniques. The focus is on greyscale images, although some aspects of colour processing are also covered.

Initially, an X-ray image is windowed and analyzed with a 3×3 window. The analysis window slides from top to bottom and left to right of the bio-image. In each 3×3 window, if the grey value of the centre pixel is non-extreme, i.e., the pixel value is neither 255 nor 0, the centre pixel is regarded as noise-free and is kept unchanged.

If the grey value is extreme, the centre pixel is regarded as potentially noisy. If all pixels in the analysis window are extreme, the window size is expanded to include more noise-free pixels. The window size is not increased when it reaches 7×7. If the values of all pixels in a 7×7 window are extreme, the grey value of the centre pixel is determined according to the majority incorporated with bias correction on the extreme pixels. On the other hand, the grey level variation of pixels is analyzed when non-extreme pixels are found in the local window. Forward and backward DWM filtering is performed in the direction with minimum variation. The smaller of the forward and backward DWM filtered values is selected as the restored grey value. To further improve the quality of the restored bio-image, block matching in a large size window is performed. The centre pixels of similar blocks are averaged to obtain the denoised pixel.

Is the centre pixel extreme?

If the answer is NO, then the selective pixels are processed and are displayed in the denoised X-ray bio-image.

If the answer is YES, then again the pixels are confirmed if they are all extreme.

If YES, then we need to further proceed with another method for filtering, namely; Extreme pixel confirmation.

3.3 Window size expansion:

We rotate around the selection of the specific segments of the total pixels value range and then select which segments show the pixel values that represent white, deep black, or grey shades, using the full brightness range from white all the way up. As an example, an 8-bit window with 1024 samples should end at 1024 by default.Windows tend to have better window sizes for filters. In math, if you are looking at a five-notch matrix with a size=5 gaussian filter, you find it to mean approximately five 5-notched matrices. Filters in discrete signal processing are generally designed to display a window length, according to their size. As a matrix window, it is used as a matrix by 2D signals like image and a vector matrix by 1D signals like audio. As all the pixels in the 3x3 matrix of grey level values are considered extreme, the size of the window is expanded to a size of 5x5 and the further verification of this window is verified to whether it is having all the pixels to extreme or not. If the same

situation arises again, i.e., all the grey values of the pixels are extreme, then again the size of the window is expanded to its next size of 7x7 matrix and this goes on…

After the expansion, the real plot is needed to be taken place which is known as "Extreme pixel confirmation".

3.4 Extreme pixel confirmation:

In digital imaging, a pixel (or picture element) is the smallest item of information in an image. Pixels are arranged in a 2-dimensional grid, represented using squares. Each pixel is a sample of an original image, where more samples typically provide more-accurate representations of the original.

Computers can use pixels to display an image, often an abstract image that represents a GUI. The resolution of this image is called the display resolution and is determined by the video card of the computer. LCD monitors also use pixels to display an image, and have a native resolution.

Each of the pixels that represents an image stored inside a computer has a pixel value which describes how bright that pixel is, and/or what colour it should be. In the simplest case of binary images, the pixel value is a 1-bit number indicating either foreground or background. Higher resolutions mean that there more pixels per inch (PPI), resulting in more pixel information and creating a high-quality, crisp image. Images with lower resolutions have fewer pixels, and if those few pixels are too large (usually when an image is stretched), they can become visible.

For a greyscale or B&W image, we have pixel values ranging from 0 to 255. The smaller numbers closer to zero represent the darker shade while the larger numbers closer to 255 represent the lighter or the white shade.

X-ray images feature many extreme pixels. The grey values of SAP noise are the same as noise-free pixels. Although using Eqns. can efficiently take out SAP noise, the extreme noise-free pixels of a bio-image may be destroyed by forward and backward DWM filtering. The quality of the restored pixel $\tilde{S}_{i,j}^{fb}$ may suffer from a greying effect if the pixel being processed is noise-free and its original grey value is 0 or 255. To prevent the noise-free and extreme pixels from deteriorating from forward and backward DWM filtering, we use the majority incorporated with bias correction on the extreme pixels to define the grey value in an analysis window, given as

$$\tilde{S}_{i,j}^{e}=\begin{cases} 0, if\ N_{i,j}^{0} \geq N_{i,j}^{255} - \sigma_{i,j} \\ 255,\ otherwise \end{cases} \text{----------(1)}$$

where $N_{i,j}^{255}$ and$N_{i,j}^{0}$in the above equation 1 respectively represent the numbers of extreme pixels with grey levels of 255 and 0. $\sigma_{i,j}$ is the bias factor falling between the numbers of pure white and pure black pixels; $\sigma_{i,j}$ is set to be ⌊ (2s + 1) 2⁄2 ⌋.

In a bio-image, organs and bones respectively appear in light or dark grey. while the background regions are pure black. In an X-ray bio-image, the number of clean pixels with pure black colour, i.e., the grey value of the pure black pixels=0, is significantly greater than that of the noise-free pixels with pure white colour, i.e., the grey value of the white pixel=255. If all pixels in an analysis window are extreme, they are more likely to be black than white. A bias correction factor between pure white and black pixels is necessary to determine colour class.

The restored pixel is expressed as:

$$\tilde{S}_{i,j}=\begin{cases}\tilde{S}_{i,j}^{fb}, & if\ N_{i,j}^{non-extrem} > 0 \\ \tilde{S}_{i,j}^{e}, & otherwise\end{cases} \text{----------(2)}$$

where $N_{i,j}^{non-extrem}$ represents the total non-extreme pixels numbers and is computed by

$$N_{i,j}^{non-extre} = \sum_{\Delta i=-s}^{s}\sum_{\Delta j=-s}^{s} F_{i+\Delta i,j+\Delta j}^{non-extre} \quad \text{---(3)}$$

where $F_{i,j}^{non-extreme}$ denotes a non-extreme flag used to denote whether the grey value of the pixel $X_{i,j}$ is non-extreme, given as

$$F_{i,j}^{non-extreme}=\begin{cases}1, & if\ X_{i,j} \neq 255\ and\ X_{i,j} \neq 0 \\ 0, & otherwise\end{cases} \text{--(4)}$$

A pixel $X_{i,j}$ is regarded as noise-free if its grey level is non-extreme. The $F_{i,j}^{non-extrem}$ is set to unity. It will be kept unchanged and is used to restore a noisy pixel. On the other hand, $F_{i,j}^{non-extrem}$ will be 0 if the grey value of the pixel $X_{i,j}$ is extreme, denoting a noise candidate.

The parameter s used to control the window size is set to (1) The corresponding window size is 3×3. If all pixels in the analysis window are extreme, the size of the window is expanded to 5×5, i.e., s is set to 2. The maximum analysis window size is 7×7. If all pixels in a 7×7 local window are still extreme, the window is considered to be in a pure black or white region. We use the majority incorporated with bias correction on the extreme pixels.

Comparing the forward and backward DWM filter, we use the restored pixel equation to determine the grey values of the restored pixels, thus preventing the restored bio-image from incurring an undesired greying effect where the pixels are either pure black or white in the original bio-image. This can significantly improve the quality of the reconstructed X-ray bio-image.

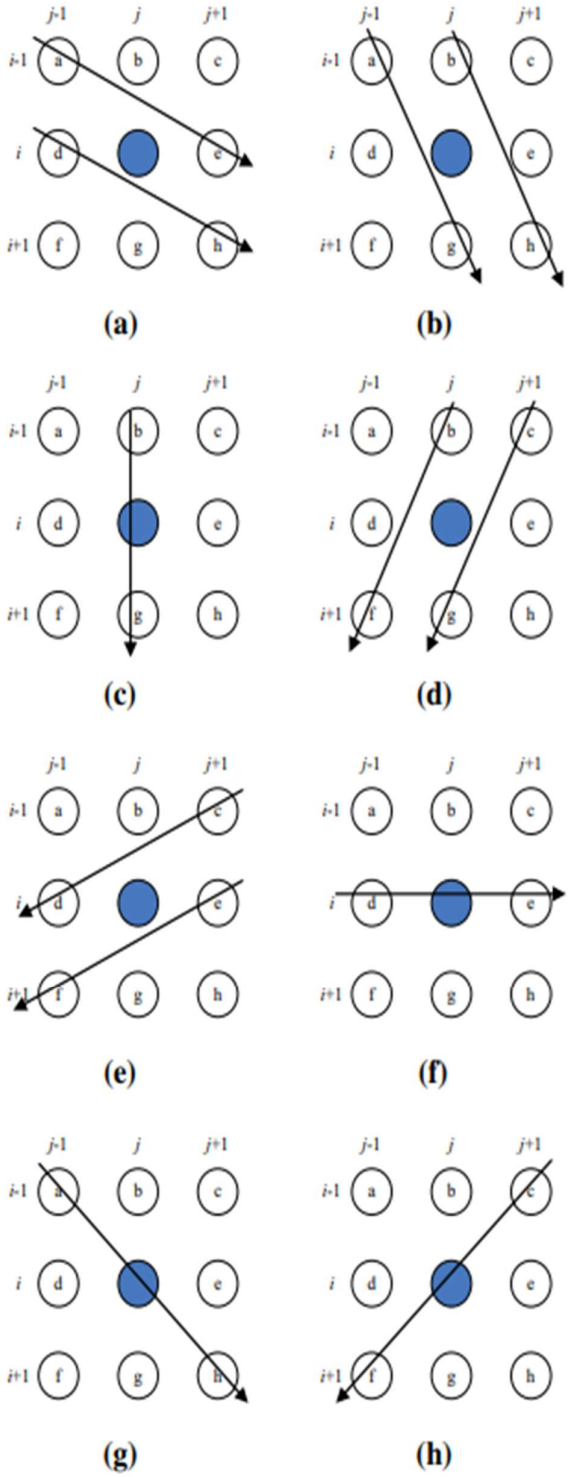

3.5 Variation direction detection:

If the grey values of the pixels are not extreme, the method of variation direction detection comes into place. The grey value of a noisy pixel is modified by the weighted median of the pixels on a selected direction with minimum variation. The DWM filter using twelve candidate directions and excluding extreme pixels for the restoration of noisy pixels. The method significantly improved DWM filter, using additional eight directions to determine the direction of pixel variation for denoising. A gradient vector represents the value's variation in a

certain direction. Here, the gradient filter gives the brightness variation in direction *X* or *Y*. When designing linear smoothing filters, the filter weights should be chosen so that the filter has a single peak, called the main lobe, and symmetry in the vertical and horizontal directions.

1/16	1/8	1/16
1/8	1/4	1/8
1/16	1/8	1/16

WHAT IS MEAN FILTERING

Mean filtering is a simple, intuitive and easy to implement method of *smoothing* images helps in reducing the amount of intensity variation between one pixel and the next. It is often used to reduce noise in images. Or simply we can say Average (or mean) filtering is a method of smoothing images by reducing the amount of intensity variation between neighbouring pixels.

Various mean filtering techniques we involve are:

Forward and backward filtering.We initiate forward and backward DWM filtering.Forward and backward DWM filtering is performed in the direction with minimum variation. The smaller of the forward and backward DWM filtered values is selected as the restored grey value. To further improve the quality of the restored bio-image, block matching in a large size window is performed. The centre pixels of similar blocks are averaged to obtain the denoised image.

3.6 **FORWARD AND BACKWARD DWM FILTER**:

A forward directional-weighted-mean (DWM) filter is used to produce a value to modify the grey level on a noise-corrupted pixel. The noisy centre pixel is replaced by the value obtained by the DWM filter which will be introduced later. Conversely. the analysis window slides

from right to left and from top to bottom for the backward DWM filter. The noise-corrupted centre pixel is replaced by the value obtained by the backward DWM filter.

Pixels with a non-extreme grey level in an analysis window can be applied to recover the noisy centre pixel. The analysis window $W_{i,j}$ is expressed as

$$W_{i,j} = \{ X_{i+\Delta i, j+\Delta j} | \; where \; \Delta i, \Delta j \; \in [-s \sim s] \} \text{ --(5)}$$

where $X_{i,j}$represents the centre pixel at the i[th] row and j[th] column of the analysis window. The window size is controlled by the parameter s, where s=1 corresponds to a 3×3 window, and s=2 corresponds to a 5×5 window, etc. In the experiments, the maximum value of s is 3. In an analysis window, only the non-extreme pixel $\tilde{X}_{i,j}$ is used to restore noisy pixels. $\tilde{X}_{i,j}$ is given as (Lu and Chou 2012)

$$\tilde{X}_{i,j} = \{ X_{i,j} \mid X_{i,j} \; \neq 255 \; and \; X_{i,j} \; \neq 0 \} \text{ -------(6)}$$

From Fig. 1, the centre pixel of an analysis window is marked by a filled circle. Pixel variation is determined by eight directional candidates. The optimum direction k∗ is selected among eight ones with the minimum pixel variation, given as (Lu et al. 2017).

$$k^* = arg \min \{ d_{i,j}^k, \quad 1 \leq k \leq 8 \} \text{ ----------(7)}$$

where k* denotes the optimum direction. $d_{i,j}^k$represents the grey level distance on the kth direction

$$d_{i,j}^1 = \begin{cases} |a-e| + |d-h|, \; if \; a,e,d,h \in \tilde{X}_{i,j} \\ d_{max}, \text{ otherwise} \end{cases} \text{ ----(8)}$$

$$d_{i,j}^2 = \begin{cases} |a-g| + |b-h|, \; if \; a,g,b,h \in \tilde{X}_{i,j} \\ d_{max}, \text{ otherwise} \end{cases} \text{ ----(9)}$$

$$d_{i,j}^3 = \begin{cases} 2.|b-g|, if \; b,g \in \tilde{X}_{i,j} \\ d_{max}, \text{ otherwise} \end{cases} \text{ ---(10)}$$

$$d_{i,j}^4 = \begin{cases} |b-f| + |c-g|, \; if \; b,f,c,g \in \tilde{X}_{i,j} \\ d_{max}, \text{ otherwise} \end{cases} \text{ ---(11)}$$

$$d_{i,j}^5 = \begin{cases} |c-d| + |e-f|, \; if \; c,d,e,f \in \tilde{X}_{i,j} \\ d_{max}, \text{ otherwise} \end{cases} \text{ ----(12)}$$

$$d_{i,j}^6 = \begin{cases} 2.|d-e|, if \; e,d \in \tilde{X}_{i,j} \\ d_{max}, \text{ otherwise} \end{cases} \text{ ----(13)}$$

$$d_{i,j}^{7}=\begin{cases}2.|a-h|, \ if\ a,h\in \tilde{X}_{i,j}\\ d_{max}, \text{otherwise}\end{cases} \quad \text{----(14)}$$

$$d_{i,j}^{8}=\begin{cases}2.|c-f|, \ if\ c,f\in \tilde{X}_{i,j}\\ d_{max}, \text{otherwise}\end{cases} \quad \text{----(15)}$$

The restored grey value of the corrupted centre pixel can be obtained by [3]

$$\tilde{S}_{i,j}^{f}=\begin{cases}\frac{a+d+e+h}{4}, if\ k^{*}=1\\ \frac{a+b+g+h}{4}, if\ k^{*}=2\\ \frac{b+g}{2}, if\ k^{*}=3\\ \frac{b+c+f+g}{4}, if\ k^{*}=4\\ \frac{c+d+e+f}{4}, if\ k^{*}=5\\ \frac{d+e}{2}, if\ k^{*}=6\\ \frac{a+h}{2}, if\ k^{*}=7\\ \frac{c+f}{2}, if\ k^{*}=8\end{cases} \quad \text{---(16)}$$

3.7 MINIMUM SELECTION

Although the forward DWM filtering method can efficiently take out corruption noise, the original black and white pixels of an X-ray bio-image may suffer from a greying effect. The computation method used for pixel restoration is similar to the forward DWM filtering method. An improved version of the restored pixel is obtained by

$$\tilde{S}_{i,j}^{fb}=\min\{\tilde{S}_{i,j}^{f},\tilde{S}_{i,j}^{b}\} \text{ ----------(17)}$$

Where $\tilde{S}_{i,j}^{b}$denotes,j the restored pixel by using Eqns. 5–17 running backward

3.8 BLOCK MATCHING

An X-ray bio-image has similar texture patches in neighbouring region. However, pixels are restored using final extreme equation which does not consider the texture properties in a region. Thus, the quality of reconstructed bio-image can be further improved.

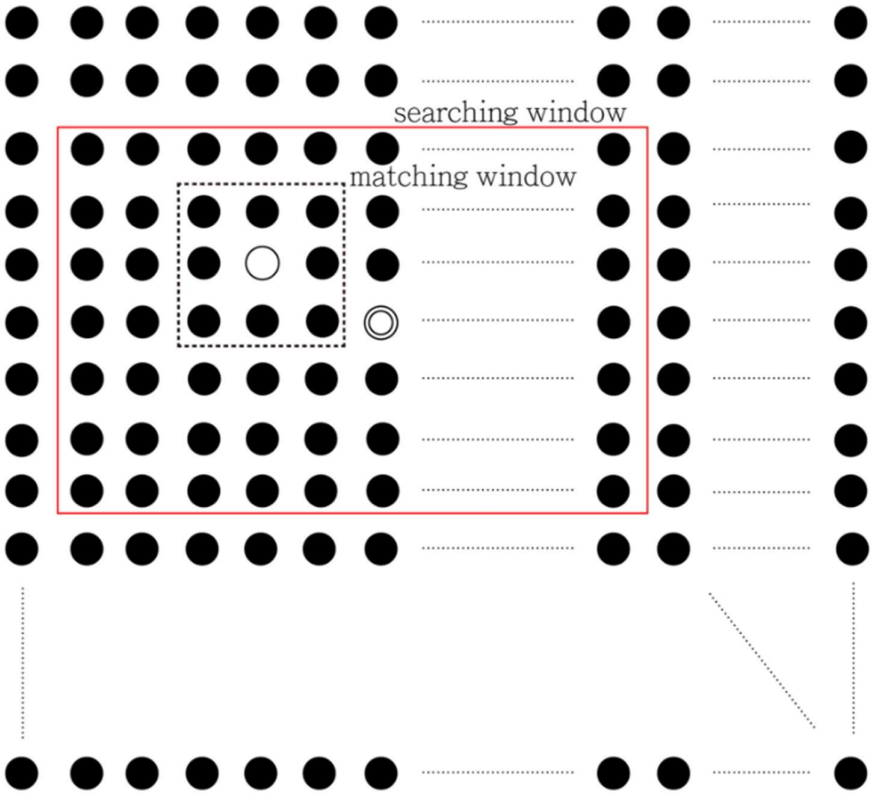

Here, a block matching refinement is performed, where the dots in diagram represent pixels in a bio-image. The centre pixel of a search window is marked as a hollow double circle. A large (27×27) search window combines similar textures. Inside the search window, a smaller matching window slides will be identified textures similar to that of the centre matching window. The centre pixel of the matching window is marked as a hollow single circle. The centre pixels of the similar matching windows are averaged to replace the restored centre pixel, thus reducing the grey level variation of pixels with similar textures and further improving the quality of the restored image.

A distance measure $d_{i,j}^{\lambda,\gamma}$ between a test matching window and the centre matching window is defined to determine whether the two matching windows are similar inside a search window. The distance $d_{i,j}^{\lambda,\gamma}$ can be expressed by

$$d_{i,j}^{\lambda,\gamma}=\sum_{\Delta\lambda=-U}^{U}\sum_{\Delta\gamma=-U}^{U}|\tilde{S}_{i+\Delta\lambda,j+\Delta\gamma}-\tilde{S}_{\lambda+\Delta\lambda,\gamma+\Delta\gamma}| \text{---------(18)}$$

where i and j respectively represent the row and column indices of the centre pixel in a search window. Δ, and γ respectively represent the row and column indices of the centre pixel in the matching window of the search window. U setups the matching window sizes; it is empirically set as 1.

If a test matching window is similar to the centre one of the search window, the distance between these two matching windows is small. Hence the similar flag $SF_{i,j}^{\lambda,\gamma}$ of the test matching window centred at λth row and γth column of the search window is set to unity. This indicates that the test matching windows centred at the λth row and γth column and at

the ith row and jth column of the search window are similar. Otherwise $SF_{i,j}^{\lambda,\gamma}$ is set to zero which indicates the test matching window is not similar to the centre matching window of the search window, given as

$$SF_{i,j}^{\lambda,\gamma} = \begin{cases} 1, if\ d_{i,j}^{\lambda,\gamma} \leq \delta_s \\ 0, otherwise \end{cases} \quad \text{----------(19)}$$

where δ_s denotes the distance threshold between two similar matching windows, and is empirically set as 3. The centre pixels of the similar matching windows are averaged to generate a post-processed grey value which is used to replace the restored pixel given in extreme pixel equation. The postprocessed pixel with block-matching $\hat{S}_{i,j}$ can be obtained by

$$\hat{S}_{i,j} = \sum_{\lambda=i-V}^{i+V} \sum_{\gamma=j-V}^{j+V} \tilde{S}_{i,j}^{\lambda,\gamma} . SF_{i,j}^{\lambda,\gamma} / \sum_{\lambda=i-V}^{i+V} \sum_{\gamma=j-V}^{j+V} SF_{i,j}^{\lambda,\gamma}$$

----(20)

where V controls the window size of search window, and is empirically set as 13, i.e., the size of the search window is 27×27. The X-ray image shows heavy interference from SAP noise (with noise density of 90%). By comparing the reconstructed X-ray image of the forward DWM filter suffers from salt residual noise near the head position and the denoised bio-image obtains a peak SNR (PSNR) of 25.69 dB. On the contrary, the denoised bioimage of the backward DWM does not suffer from this kind of residual noise. The PSNR of the denoised bio-image equals 25.68 dB. Using the minimum grey-value of the forward and backward filtering pixel can prevent this salt residual noise. The output bio-image achieves a PSNR of 25.89 dB. In addition, as shown in Fig. 4c, the denoised bio-image of the forward DWM filter suffers from a Greying effect. As shown in Fig. 4d, the denoised bio-image of the backward DWM filter suffers from a Greying effect on the right-hand side. This greyed effect can be efficiently mitigated by selecting the minimum Grey value of the forward and backward DWM filtering pixels. Finally, the quality of the reconstructed X-ray image is further improved by averaging similar blocks in a search window, as shown in Fig. 4f. The output of the PSNR is 25.93 dB. [4] Although the size of search window given in Eq. (20) is very large (i.e., 27×27), the post-processed bio-image does not suffer from blurring because the value of the distance threshold δ_s between two similar matching windows is very small. Only highly correlated matching windows are averaged to determine the post-processed value of the Grey level. Consequently, as shown in Fig. 4f, the post-processed bio-image is free from blurring.

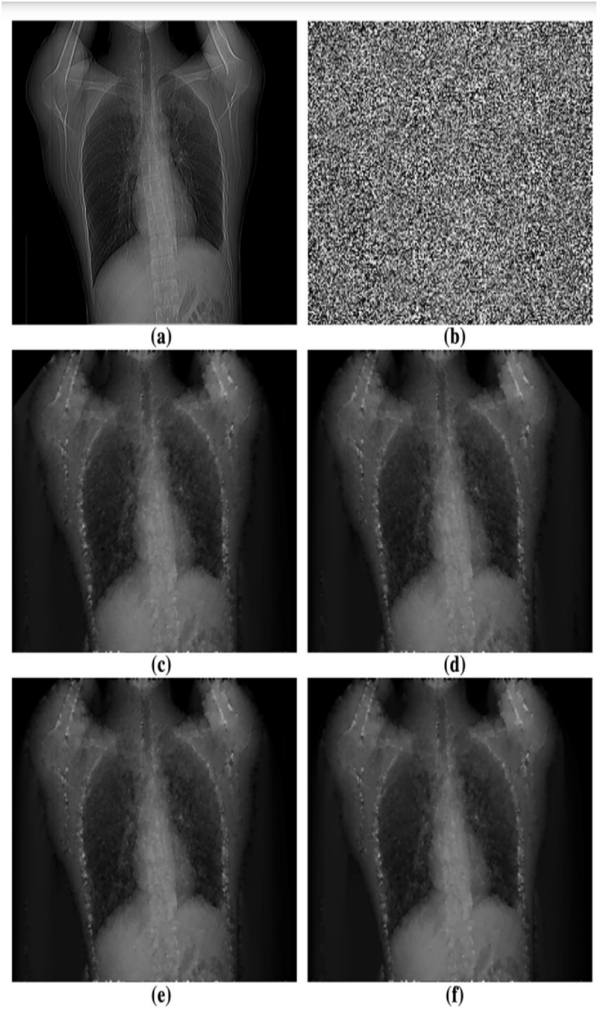

Figure 4

4.1 Experimental Results

Test X-ray images were used to measure the performance of the proposed image restoration method. The test X-ray images are with the sizes 512×512 and 512×512, and exhibited different SAP noise density levels up to 60%. Performance was compared using the switch median (SM) filter, the DWM filter [5], the MDBUTM filter [6], the modified DWM (MDWM) filter [7], and the distance-based algorithm (DBA) [8]. The quality of denoised bio-images was measured using the mean-structural-similarity (MSSIM) index (Wang et al. 2004) and the peak signal-to-noise ratio (PSNR).

5.1 PSNR measure

The PSNR is widely used to measure image quality, and was used here to estimate the character of reconstructed X-ray images, given as

$$PSNR(dB) = 10 \cdot \log_{10} (E_{max}/E_{MSE}) \text{----(21)}$$

where E_{max} is the maximum energy of the grey level, and setups 255^2 for an 8-bit grey level image. E_{MSE} represents the mean-square-error between the original clean and the restored bio-images

The performance comparison of the various restoration approaches are show in Tables 1 and 2. A larger PSNR value represents better reconstructed bioimage quality. These results demonstrate that the proposed approach outperforms the others in terms of noise removal and image restoration. The results illustrated when the noise density exceeds 70%, SM, MDBUTM and DWM filter performance decays dramatically, and only the MDWM filter, DBA and the proposed methods can successfully reconstruct the heavy noise-corrupted bio-images. Table 2 compares performance for the Chest2 bio-image. The proposed method has the better performance under most noise corruption conditions with noise densities ranging from 0 to 60%. Given noise density of 10%, the DWM filter has slightly better performance than the proposed method. For the Chest2 bio-image, the proposed method has better performance than other methods when noise density exceeds 70%. By comparing the performance presented in Tables 1 and 2, the MDWM filter and the DBA method are better able to recover the Chest1 bio-image. However, these two methods cannot rebuild the Chest2 X-ray image very well because the clean Chest2 X-ray image has many extreme pixels where the grey levels of the noise-free pixels are the same as the interference noise. Conversely, the proposed method can efficiently restore both the Chest2 and Chest1 X-ray images, confirming that the proposed approach is better able to reconstruct bio-images than the other methods given various noise densities.

5.2 Mean-structural-similarity index measure:

This experiment is indicated by a mean-structural-similarity (MSSIM) index to calculate the difference between original clean bio-image and reconstructed bio-image (Wang et al. 2004),

The value of MSSIM ranges from 0 to 1. The lower value of the MSSIM denotes the worse quality of the reconstructed bio-image. The performance comparisons for the various methods are shown in Tables 3 and 4. From Table 3, the DBA method has the significant performance in light noise corruption conditions with noise density ranging from 10 to 40% for the Chest1 bio-image. The performance of the proposed method is close to that of the DBA method. The proposed method provides the highest MSSIM scores of all methods when the noise density exceeds 50%. These results confirm that the proposed approach efficiently preserves the body tissue structures in the restored bio-image while removing SAP noise. In Table 4, the DWM filter slightly has better performance than the proposed approach in light and middle noisecorruption conditions with noise density below 60%. This is attributed to the DWM filter being better able to restore the texture in light and middle noise-corruption

conditions. Heavy noise corruption (i.e., noise density exceeding 70%) dramatically reduces the performance of the DWM, SM, MDWM, and MDBUTM filters. Only the proposed and the DBA methods can still take out SAP noise efficiently, while efficiently preserving the detailed texture of body tissue. The proposed method outperforms the DBA method in all noise corruption conditions.

6 Reconstructed Images:

Figures 1,2 and 3 illustrate the reconstructed bio images of the various methods for the Chest1 and Chest2 bio-images with noise densities of 10, 20, 30, 40, 50 and 60%. In Fig. 1, the original Chest1 X-ray images is subject to SAP noise with a 10% noise density. All methods are found to efficiently

take out SAP noise and preserve textural details, such as the ribs, brain and knee. In the Chest1 bio-image is subject to SAP noise with a 50% noise density. Plenty of residual noise exists in the restored X-ray image denoised using the SM filter providing the worst performance of all the considered methods. The DWM filter, the MDBUTM filter, the MDWM filter, the DBA method, and the proposed approach can all efficiently preserve body tissue particularly around the ribs. The restored bio-images of the MDBUTM filter (Fig. 6e) and the MDWM filter (Fig. 6f) show some residual noise at the bottom of the restored bio image, and denoising should be further improved. The proposed approach (Fig. 6h) and the DBA method (Fig. 6g) not only efficiently take out SAP noise, but also preserve bioimage textures, such as the ribs. Accordingly, the proposed scheme and the DBA method outperform the other methods.

7.1 PSNR Values of Various methods that performed:

S.no	*Type of X-Ray Image*	*Noise Density*	*MDBUTM*	*DBA*		*DWM*	*Obtained*
1	Pneumonia	10	32.055	31.6157		30.8156	38.9698
2	Pneumonia	20	28.2753	27.6307		27.7687	37.7633
3	Pneumonia	30	25.6154	24.2577		25.1955	35.8431
4	Pneumonia	40	23.7597	21.6042		23.3782	34.745
5	Pneumonia	50	21.9951	19.4012		21.4545	32.1451
6	Pneumonia	60	20.4454	17.5054		19.4891	28.2868
7	Knee	10	46.8886	30.3548		32.1486	49.4616
8	Knee	20	43.0498	27.3794		29.1339	45.6271
9	Knee	30	40.4353	24.4565		26.9632	42.2774
10	Knee	40	38.3946	21.3449		25.2093	40.2407
11	Knee	50	33.9702	19.0417		23.4061	36.3538
12	Knee	60	28.2324	17.0868		21.2879	30.2935
13	Brain	10	27.5192	28.1697		29.315	39.7554
14	Brain	20	23.344	23.3752		25.1842	37.5971
15	Brain	30	20.7176	19.9245		22.638	35.2729
16	Brain	40	18.6498	17.3734		20.3905	33.0464
17	Brain	50	17.0473	15.145		18.5083	30.7051
18	Brain	60	15.491	13.3522		16.659	26.9321

7.2 SSIM values of Various methods that performed:

S.no	*Type of X-Ray Image*	*Noise Density*	*MDBUTM*	*DBA*	*DWM*	*Obtained*
1	Pneumonia	10	0.9258	0.7893	0.9215	0.9897
2	Pneumonia	20	0.9111	0.6723	0.8987	0.9778
3	Pneumonia	30	0.9008	0.5518	0.8697	0.9627
4	Pneumonia	40	0.8873	0.4572	0.8029	0.9401
5	Pneumonia	50	0.8538	0.3829	0.6762	0.9031
6	Pneumonia	60	0.7627	0.3292	0.4867	0.8244
7	Knee	10	0.9913	0.7603	0.9755	0.992
8	Knee	20	0.9811	0.635	0.9611	0.9817
9	Knee	30	0.9686	0.5099	0.9291	0.9681
10	Knee	40	0.9512	0.3853	0.844	0.9496
11	Knee	50	0.91	0.321	0.687	0.9194
12	Knee	60	0.7919	0.2512	0.4609	0.8387
13	Brain	10	0.7787	0.5393	0.7891	0.9889
14	Brain	20	0.745	0.365	0.75	0.9784
15	Brain	30	0.7318	0.2583	0.7229	0.9646
16	Brain	40	0.7116	0.1895	0.6663	0.9461
17	Brain	50	0.6686	0.1434	0.5607	0.9157
18	Brain	60	0.5706	0.112	0.404	0.8533

Experimental output images of Pneumonia :

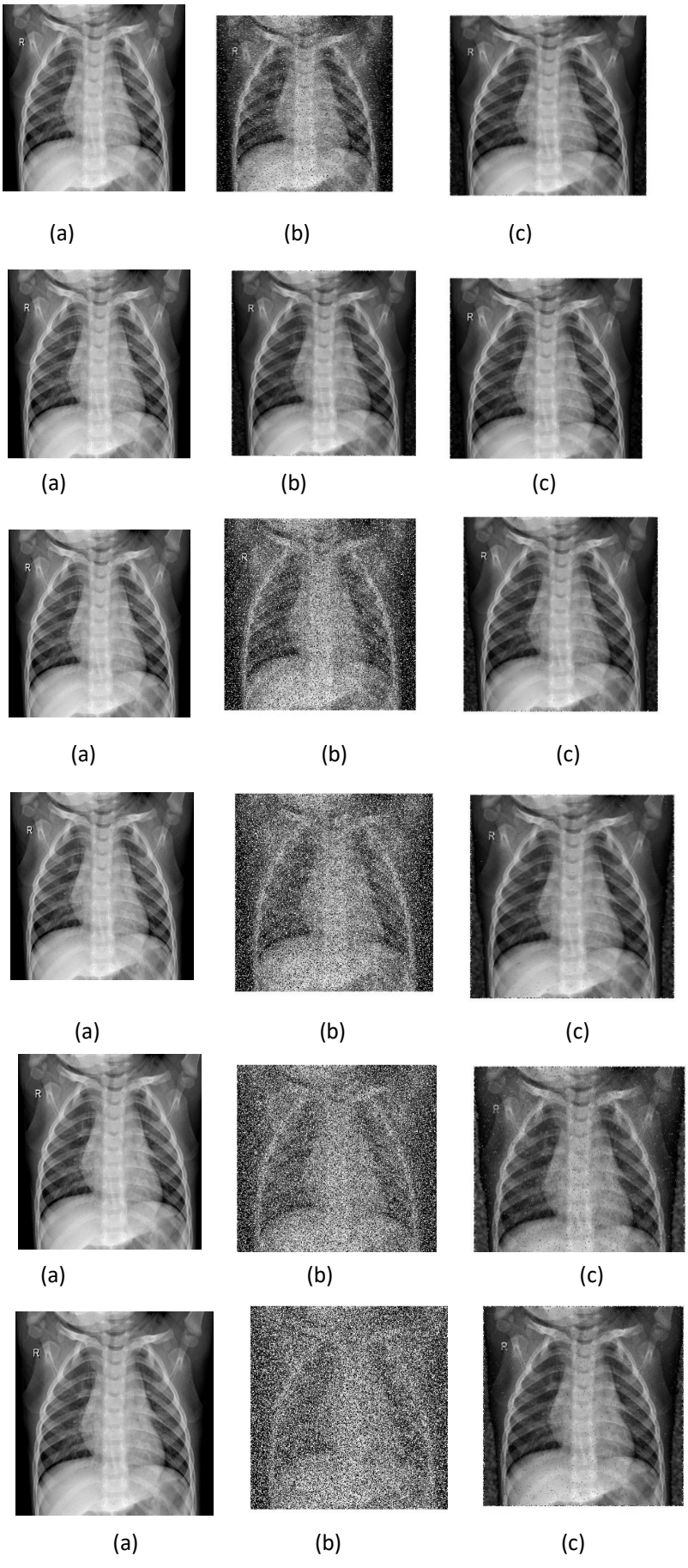

Fig.1 Restored X-ray bioimages of compared approaches for the X-ray bio-image with different noise density levels from 10% to 60% in the image (b)

Experimental output images of Brain :

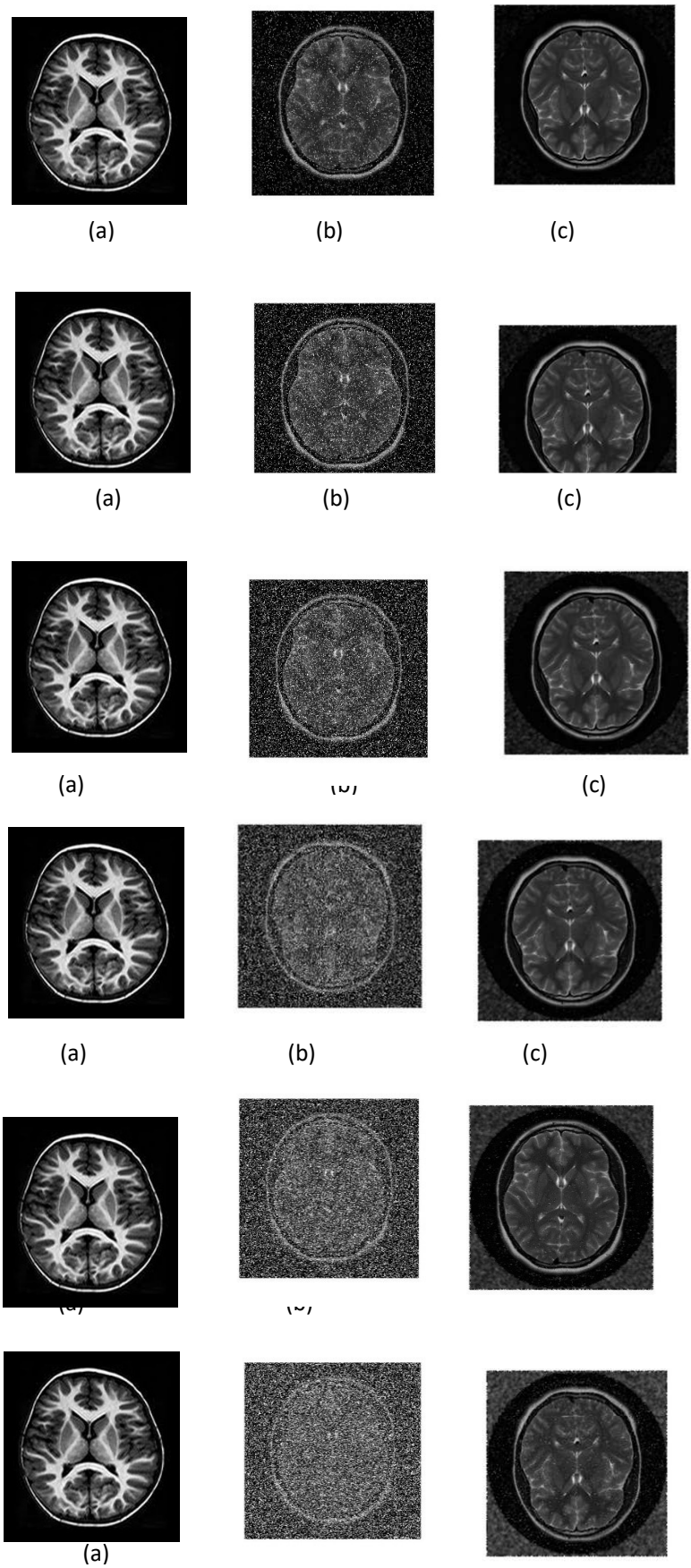

Fig.3 Restored X-ray bio images of compared approaches for the X-ray bio-image with different noise density levels from 10% to 60% in the image (b)

Experimental output images of Knee :

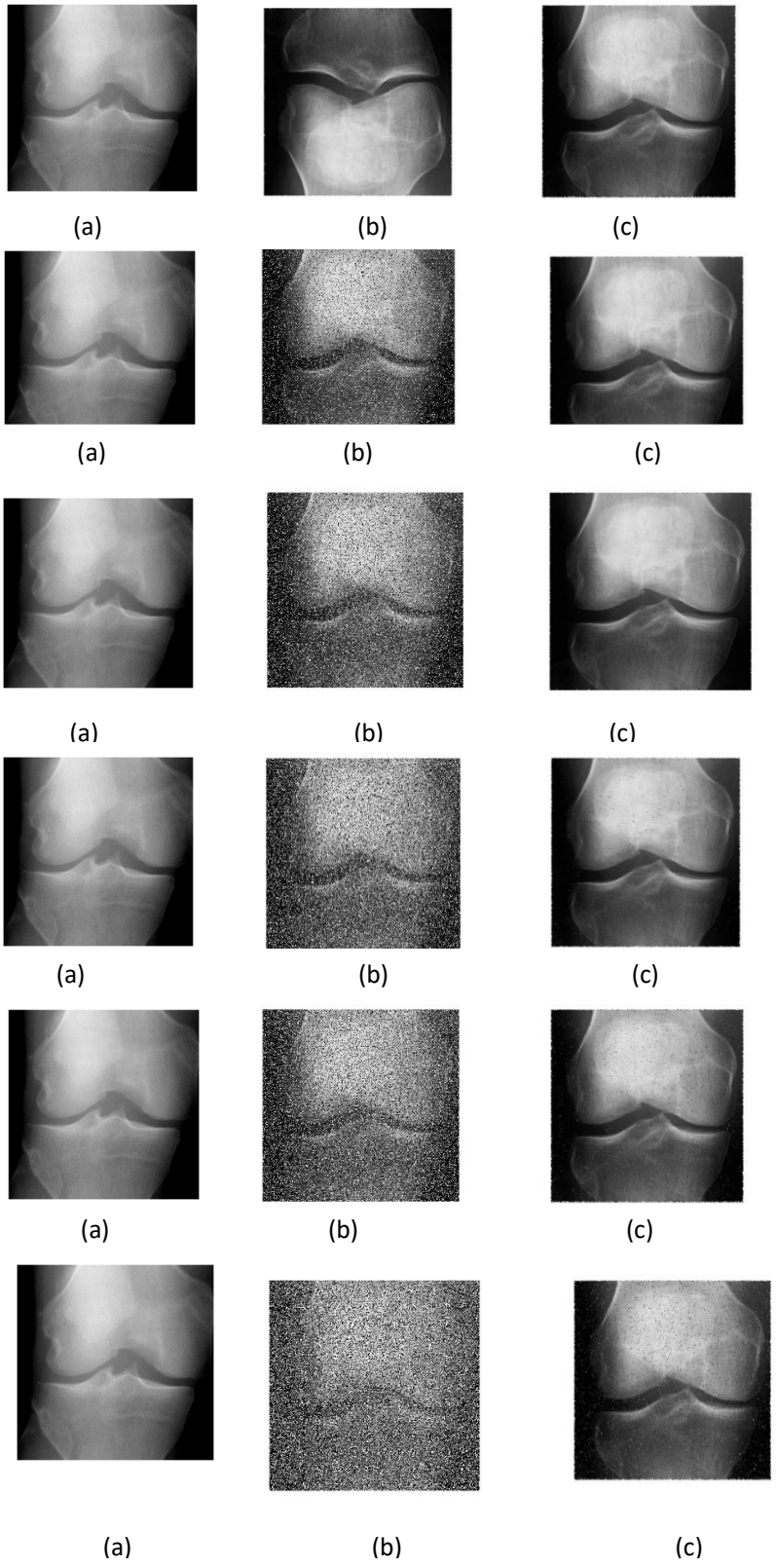

Fig.2 Restored X-ray bioimages of compared approaches for the X-ray bio-image with different noise density levels from 10% to 60% in the image (b)

In Fig. 7b, the Chest2 X-ray image is subject to SAP noise with a 50% noise density. Figure 7a shows numerous of black and white pixels in the original noise-free bio-images. The grey levels of these pixels are identical to SAP noise, which is difficult to take out from noise corrupted bio-images. In Fig. 7c, the SM filter cannot efficiently restore the X-ray image due to the presence of excessive white pixels in the restored X-ray image, producing the worst performance of all compared approaches. The DWM filter (Fig. 7d), the MDBUTM filter (Fig. 7e), the MDWM filter (Fig. 7f), the DBA method (Fig. 7g), and the proposed approach (Fig. 7h) can efficiently denoise corruption noise. However, the denoised bio-image of the DWM filter (Fig. 7d) suffers from serious blurring at the ribs and humerus, producing unacceptable image quality. The MDBUTM filter (Fig. 7e), the MDWM filter (Fig. 7f), and the DBA method (Fig. 7g) efficiently restore body tissue texture. However, significant levels of residual noise are still present in the peripheral body tissue, where the X-ray bio-image is presented by black pixels. The peripheral tissue at the top-left corner of the DBA method (Fig. 7g) also suffers from residual noise. The proposed approach (Fig. 7h) can not only efficiently take out such interference noise, but also can efficiently restore these peripheral areas. In Fig. 8b, the Chest1 bio-image is heavily interfered with by SAP noise with an 80% noise density, and the SM filter fails to restore the image (Fig. 8c), while reconstruction with the DWM filter produces serious blurring. The proposed approach (Fig. 8h), the MDBUTM filter (Fig. 8e), the MDWM filter (Fig. 8f), and the DBA method (Fig. 8g) can efficiently restore the X-ray image texture. However, too much residual noise in the restored image is denoised by the MDBUTM filter (Fig. 8e), thus reducing image quality. The reconstructed X-ray images at the ribs are not smooth enough for the MDWM filter (Fig. 8f) or the DBA method (Fig. 8g). Accordingly, the quality of the proposed method has the significant improvement and performance. In Fig. 9b, the Chest2 bio-image is heavily corrupted by SAP noise with an 80% noise density. The SM filter (Fig. 9c) and the DWM filter completely fail to restore this bio-image. The MDBUTM filter efficiently restores the body tissue outline (Fig. 9e), but the reconstructed X-ray image suffers from serious residual noise, significantly reducing quality particular in areas with dark pixels. Only the proposed method (Fig. 9h), the MDWM filter (Fig. 9f), and the DBA method (Fig. 9g) efficiently restore this Chest2 X-ray image. However, the MDWM filter (Fig. 9(f)) suffers from a greying effect at peripheral body tissue. The DBA method (Fig. 9g) suffers from residual noise at the top-left corner of the restored image. The proposed method can efficiently take out interference noise and provides significantly better reconstruction of bone edge details, such as at the arms and chest. In addition, the proposed approach can adequately restore the extreme pixels where the noise-free pixels are pure black.

8.1 Discussions:

In Table 2, the PSNR measure of the Chest2 X-ray image has the better performance than other state-of-art methodologies. In Table 4, it has also better performance to the other approaches in terms of the MSSIM given noise density exceeding 70%. The proposed approach is thus better able to take out corruption noise than the other methods for noise density ranging from 20 to 90%. However, the quality of the reconstructed bio-image of the proposed method is comparable to the DBA method. With a noise corruption density exceeding 70%, the proposed approach significantly outperforms the other three approaches in bio-image reconstruction while efficiently removing corruption noise. In Table 3, the proposed method outperforms the other approaches for noise densities exceeding 50%. But in Table 4, the proposed method does not outperform the DWM filter for noise density levels below 60%. It maybe causes from the number of noise-free and non-extreme neighbour pixels is sufficient for the DWM filter to efficiently reconstruct and restore noisy pixels. Accordingly, the DWM filter obtains higher MSSIM scores than the proposed method for low noise density corruption. However, when noise density exceeds 70%, the number of clean and non-extreme pixels is insufficient for effective DWM filter restoration of the noisy bio-image. Accordingly, the proposed approach achieves much higher MSSIM scores than the other methods. In Fig. 9b, the Chest2 bio-image is heavily interfered with by SAP noise with an 80% noise density level. The textures and the edges of the bio-image are significantly degraded, so the structure of the original bio-image cannot be distinguished. The proposed approach can efficiently restore the textures and edges, as shown in Fig. 9h, mainly because the proposed method uses non-extreme pixels to reconstruct noisy pixels in the forward and backward DWM filters, as shown in Eqns. (1)–(12), allowing for extensive removal of the background. In addition, the greying effect of the reconstructed bio-image can be mitigated by selecting the minimum filtered value, obtained by the forward and backward DWM filters as given in Eq. (13), to replace the centre noise-corrupted pixel of an analysis window. Although the proposed method can efficiently reconstruct a significantly noise corrupted bio-image in the spatial domain, it can extract robust features in the restored bio-image for performance improvement, such as through pattern recognition applications (Samuel et al. 2017a). In addition, the denoised bio-image could be further improved using a post processor based on machine learning (Liang et al. 2017) or artificial neural networks with fuzzy decision methods (Samuel et al. 2017b).

8.2 References:

[1] Ahmed F,Das S (2014) Removal of high density salt-and-pepper noise in images with an iterative adaptive fuzzy filter using alphatrimmed mean. IEEE Trans Fuzzy Syst 22(5):1352–1358

[2] Bhadauria HS, Dewal ML (2013) Medical image denoising using adaptive fusion of curvelet transform and total variation. ComputElectrEng 39(5):1451–1460

[3] Chen PY, Lien CY (2008) An efficient edge-preserving algorithm for removal of salt-and-pepper noise. IEEE Signal Process Lett 14:833–836

[4]Deivalakshmi S, Palanisamy P (2016) Removal of high density salt and pepper noise through improved tolerance based selective arithmetic mean filtering with wavelet thresholding. Int J Electron Commun (AEU) 70(6):757–776

[5]Dong YQ, Xu SF (2007) A new directional weighted median filter for removal of random-valued impulse noise. IEEE Signal Process Lett 14(3):31–34

[6] EsakkirajanS,Veerakumar T, Subramanyam AN, PremChand CH (2011) Removal of high density salt and pepper noise through modified decision based unsymmetric trimmed median filter. IEEE Signal Process Lett 18(5):287–290

[7]Lu CT, Chou TC (2012) Denoising of salt-and-pepper noise corrupted image using modified directional-weighted-median filter. Pattern Recognit Lett 2012 33(10):1287–1295

[8] Ravi Teja KV, Shanmukha Rao N, Santhosh Kumar P (2017) Distance based algorithm for removal of salt and pepper noise. In: Proceedings of the IEEE International conference on circuit, power and computing technologies.